MODELLING TURBULENT FILM FLOW

Peter S. Johansson, Helge I. Andersson, Robbert Fortunati*
Department of Applied Mechanics, Thermodynamics and Fluid Dynamics, NTNU
7491 Trondheim, Norway
peterj@mtf.ntnu.no, helge.i.andersson@mtf.ntnu.no, r.fortunati@siep.shell.com

ABSTRACT

Turbulence in the vicinity of a zero mean-shear gas-liquid interface is considered using low-Reynolds-number second-moment closure modelling. Near-boundary damping is achieved by elliptic relaxation, which has proved to be particularly amenable to mimic the turbulence anisotropy near solid surfaces. A modification of the elliptic relaxation formulation and the accompanying length scale is proposed to improve the behaviour of the redistribution term in the vicinity of the free surface without deteriorating its wall characteristics. The new formulation is verified against DNS data of channel flow and experiments on film flow. The wall-friction dependence on Reynolds number is compared with experimental data, a mixing-length formulation, the Launder & Sharma k-ε model and Durbin's k-ε-v^2 model. The full Reynolds stress model and the k-ε-v^2 model compare most favourably with the experimental results.

INTRODUCTION

Turbulence modelling is essential in computerised flow analysis and turbulence closures are normally developed and tested for either free or wall-bounded flows. However, numerous industrial applications, notably in chemical engineering, involve flow problems in which the turbulence adjacent to a gas-liquid interface plays a crucial role in the determination of interfacial transport processes; see e.g. Fulford (1964).

In this paper we consider gravity driven flow of a thin liquid film down along a vertical wall, as depicted in figure 1. It is commonly assumed that the flow becomes turbulent when the film Reynolds number, $Re = q/\nu$, exceeds 400. Here, q denotes the volumetric flow rate per unit width of the film and ν is the kinematic viscosity of the liquid. Alekseenko et al. (1994), however, claim that transition to turbulence takes place somewhere in the range $500 < Re < 1000$.

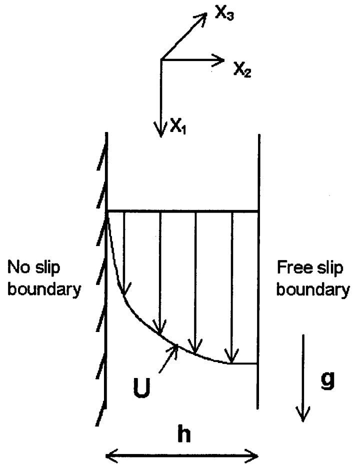

Figure 1: Sketch of the flow geometry with coordinate system and mean velocity profile.

THE PHYSICAL PROBLEM

Let us for simplicity assume that the turbulent film flow under consideration here is statistically steady and fully developed in the streamwise (i.e. vertical) direction and that the wave-free interface is maintained parallel to the wall. The friction against the surrounding gas phase is assumed negligible and the liquid flow is therefore driven solely by the gravitational acceleration g. The one-dimensional mean flow $U(x_2)$ is governed by the Reynolds-averaged Navier-Stokes equations, which readily can be integrated once to give a linear variation of the total shear stress

$$\nu\frac{dU}{dx_2} - \overline{u_1u_2} = -gx_2 + u_*^2 \qquad (1)$$

from the wall (x_2=0) to the free surface (x_2 =h). Here, u_* denotes the conventional wall friction velocity, which in this particular situation relates directly to the film thickness h according to $u_*^2 = gh$, since both sides of equation (1) should vanish at the interface.

*exchange student from J.M. Burgers Centre, Laboratory for Aero- and Hydrodynamics, TU Delft, 2628 AL Delft, The Netherlands

TURBULENCE MODELLING

The crucial question which now remains to be addressed is how to model the kinematic Reynolds shear stress in equation (1). If a mixing-length type of model is adopted, the closed form solution

$$U(y) = \int_0^y \frac{2(h-y)g/\nu}{1+(1+4(h-y)gl^2/\nu^2)^{1/2}}dy \quad (2)$$

is readily obtained, where van Driest's (1956) representation of the mixing-length l can be expected to be reliable near the wall and a number of modifications can be applied further out; see e.g. Yih & Liu (1983) for an overview.

However, physical intuition suggests that the turbulence in the vicinity of a shear free boundary is highly anisotropic and approaches a two-dimensional state at the surface itself. Accordingly, all turbulence models based on Boussinesq's eddy viscosity hypothesis, including algebraic mixing-length models and differential k-ε models, inevitably fail to return a non-isotropic Reynolds stress field at a shear-free surface.

To this end a differential second-moment closure (SMC) is adopted, as advocated by Gibson & Rodi (1989) for open-channel flow. While they used a so called wall-proximity function in order to weaken the effect of the pressure-strain redistribution near the solid and free surface, the elliptic relaxation formalism devised by Durbin (1993) eliminates the need for wall-distances and wall-normals. In this novel approach, a relaxed pressure-strain tensor, $\wp_{ij} = k \cdot f_{ij}$, is introduced and related to an intermediate tensorial variable f_{ij}, the latter which in turn is obtained from a Helmholtz type elliptic equation

$$L^2\nabla^2 f_{ij} - f_{ij} = -\phi_{ij}^h/k \quad (3)$$

where ϕ_{ij}^h is a homogeneous pressure-strain model. By multiplying f_{ij} with the turbulent kinetic energy, k, the correct behaviour of $\wp_{ij} \to 0$ at a no-slip boundary is enforced. Note that $\wp_{ij}$ represents both the pressure-strain and the redistributive part of the pressure diffusion term.

Furthermore Durbin (1993) included the misalignment of the dissipation tensor and the Reynolds stress tensor into $\wp_{ij}$. The effect of this is that the dissipation will be represented by the term $\frac{\overline{u_iu_j}}{k}\varepsilon$ close to the wall and the term $\frac{2}{3}\delta_{ij}\,\varepsilon$ in the quasi-homogeneous limit, that is far from walls. (Another way of interpreting this is that $\overline{u_iu_j}\frac{\varepsilon}{k}$ represents ε_{ij} everywhere and that the return-to-isotropy constant is reduced by 1 to account for the dissipation being modelled anisotropic in contrast to conventional turbulence modelling.) With these presuppositions the Reynolds stress transport equations become

$$D_t\overline{u_iu_j} = P_{ij} + \wp_{ij} - \overline{u_iu_j}\frac{\varepsilon}{k} + T_{ij} + \nu\nabla^2\overline{u_iu_j} \quad (4)$$

where

$$\begin{aligned} P_{ij} &= -\overline{u_iu_k}\,\partial_k U_j - \overline{u_ju_k}\,\partial_k U_i \\ \wp_{ij} &= -\overline{u_i\partial_j p} - \overline{u_j\partial_i p} + \frac{2}{3}\overline{u_k\partial_k p}\,\delta_{ij} \quad (5) \\ &\quad -(\varepsilon_{ij} - \overline{u_iu_j}\frac{\varepsilon}{k}) \\ T_{ij} &= -\partial_k(\overline{u_ku_iu_j} + \frac{2}{3}\overline{u_kp}\,\delta_{ij}) \\ \varepsilon_{ij} &= \frac{2}{3}\delta_{ij}\,\varepsilon \end{aligned}$$

Turbulent diffusion is modelled according to Daly-Harlow (1970) as

$$T_{ij} = \partial_l(C_\mu\overline{u_lu_m}\;T\,\partial_m\overline{u_iu_j}) \quad (6)$$

The elliptic relaxation equation then becomes

$$L^2\nabla^2 f_{ij} - f_{ij} = -\frac{\phi_{ij}^h}{k} - \frac{\overline{u_iu_j} - \frac{2}{3}k\,\delta_{ij}}{kT} \quad (7)$$

Durbin (1993) defined the time scale and the elliptic length scale as

$$T = \max\left[\frac{k}{\varepsilon},\; C_T(\frac{\nu}{\varepsilon})^{1/2}\right] \quad (8)$$

$$L = C_L \max\left[\frac{k^{3/2}}{\varepsilon},\; C_\eta(\frac{\nu^3}{\varepsilon})^{1/4}\right] \quad (9)$$

In this way the Kolmogorov scales represent a lower bound on the time and length scales, and singularities at the wall are avoided.

Modification of the elliptic relaxation formulation for a free surface

As mentioned earlier, the turbulent kinetic energy, k, multiplied with f_{ij} assures that $\wp_{ij} = 0$ at a no-slip wall. At a free surface, k is not zero. This means that imposing blocking on the normal component gives $\wp_{22} \neq 0$ at the free surface, which is physically wrong. To evade this $\wp_{ij}$ is redefined in a manner similar to Dreeben & Pope (1997)

$$\begin{aligned} \wp_{ij} &= f_{ij}\,|u_iu_j|^{1/2} - \frac{\delta_{ij}}{3}(f_{11}\,|u_1u_1|^{1/2} \\ &+ f_{22}\,|u_2u_2|^{1/2} + f_{33}\,|u_3u_3|^{1/2}) \quad (10) \end{aligned}$$

This formulation[1] enforces $\wp_{22} = 0$ on the free surface and satisfies the redistribution property $\wp_{11} + \wp_{22} + \wp_{33} = 0$. $\wp_{ij}$ is bridged from the quasihomogeneous solution to the proper boundary value through the modified elliptic equation[1] given as

$$L^2\nabla^2 f_{ij} - f_{ij} = -\frac{\phi_{ij}^h}{|u_i u_j|^{1/2}} - \frac{\overline{u_i u_j} - \frac{2}{3}k\,\delta_{ij}}{|u_i u_j|^{1/2} T} \quad (11)$$

The dissipation of turbulent kinetic energy is found from the transport equation,

$$D_t\varepsilon = \frac{C_{\varepsilon 1}^* P_k - C_{\varepsilon 2}\varepsilon}{T} + \partial_k\left[(\nu + \frac{\nu_{T_{kl}}}{\sigma_\varepsilon})\partial_l\varepsilon\right] \quad (12)$$

where $\nu_{T_{kl}} = C_\nu \overline{u_k u_l} T$. $C_{\varepsilon 1}^* = C_{\varepsilon 1}(1 + a_1 P_k/\varepsilon)$ is made dependent of P_k (Durbin, 1993) in order to increase the dissipation close to the wall.

Quasi homogeneous pressure-strain model

The SSG model (Speziale et al., 1991) is employed as quasihomogeneous pressure-strain model. (The model is not presented here.) All original constants, except g_3^* are retained. Wizman et al. (1996) found better agreement with DNS in the log-layer by increasing g_3^* from 1.3 to 1.5. These observations were confirmed in our simulations, and $g_3^* = 1.5$ was therefore adopted in this study.

Boundary conditions

Boundary conditions for f_{ij} at the wall are obtained by studying the leading terms in the Reynolds stress transport equation approaching the wall assuming $\overline{u_1^2}$ and $\overline{u_3^2} \propto x_2^2$, $\overline{u_2^2} \propto x_2^4$, $\overline{u_1 u_2} \propto x_2^3$ and $\varepsilon_{wall} = 2\nu k_{,1}/x_{2,1}^2$. (The notation ,1 means that the variable is evaluated at the first grid point away from the boundary.) This gives

$$\begin{aligned} f_{11w} &= f_{33w} = 0 \\ f_{22w} &= -\frac{10\nu}{x_{2,1}^2}|u_2 u_2|_{,1}^{1/2} \\ f_{12w} &= \frac{4\nu}{x_{2,1}^2}|u_1 u_2|_{,1}^{1/2} \end{aligned} \quad (13)$$

For the velocity we use the usual no-slip conditions

$$U_1 = 0,\ \overline{u_1^2} = \overline{u_2^2} = \overline{u_3^2} = 0 \quad (14)$$

Following the same procedure for the free surface assuming $\overline{u_1^2}$, $\overline{u_3^2}$ and $k \simeq$ constant, $\overline{u_2^2} \propto x_2^2$ and $\overline{u_1 u_2} \propto x_2$, boundary values at the free surface become

$$f_{22s} = -\frac{2\nu}{x_{2,1}^2}|u_2 u_2|_{,1}^{1/2} \quad (15)$$

For f_{11s}, f_{33s} and f_{12s} we choose

$$\begin{aligned} \partial_2 f_{11s} &= 0 \\ f_{33s} &= -f_{11s}\left|\frac{u_1 u_1}{u_3 u_3}\right|_{,0}^{1/2} \\ f_{12s} &= \frac{0.2\nu}{x_{2,1}^2}|u_1 u_2|_{,1}^{1/2} \end{aligned} \quad (16)$$

The free surface is modelled as a free-slip surface, neglecting shear to ambient fluid and normal motion of the surface

$$\partial_2 U_1 = 0,\ \partial_2\overline{u_1^2} = \partial_2\overline{u_3^2} = 0,\ \overline{u_2^2} = 0 \quad (17)$$

$\wp_{11}$ is set equal to $-\wp_{33}$ at the surface. This assures that the trace of $\wp_{ij}$ is zero and that $\wp_{22} = 0$. If also the derivative of f_{33} is set to zero, both f_{11} and f_{33} will be negative since $\overline{u_2 u_2}$ is zero. The quasihomogeneous pressure-strain model normally redistributes energy to $\overline{u_2 u_2}$ from both the streamwise and spanwise component. f_{33} is set positive since $\overline{u_3 u_3}$ is smaller than $\overline{u_1 u_1}$. Energy is thereby transfered from the streamwise component to the spanwise component at the surface. Assuming $\overline{u_1 u_2} \propto x_2$, the near-surface analysis gives $f_{12s} = 0$, i.e. there should be no blocking of $\overline{u_1 u_2}$. If this is implemented, the velocity attains a maximum below the free surface even at $Re_\tau = 180$. This feature is not shown in DNS of film flow at this Reynolds number (Lam & Banerjee, 1992). Therefore $\frac{1}{10}$ of the blocking coefficient for $\overline{u_2 u_2}$ is adopted for $\overline{u_1 u_2}$.

Modified elliptic length scale

If the original length scale (eq. 9) is employed, the damping of $\overline{u_2 u_2}$ towards the surface will become too strong since L here is large due to small dissipation, ε. The elliptic length scale needs to be reduced substantially towards the surface to achieve the right blocking of $\overline{u_2 u_2}$. Also in channel flow, L has to be reduced in the centre of the channel to decrease the effect of the elliptic operator. If this is not done, $\overline{u_3 u_3}$ will be larger than $\overline{u_1 u_1}$ in the channel centre, see Durbin (1993). The length scale used here, both for the channel flow and the film flow simulation is

$$L = C_L \frac{\max\left[\frac{k^{3/2}}{\varepsilon},\ C_\eta(\frac{\nu^3}{\varepsilon})^{1/4}\right]}{1 + \max\left[0, C_s\frac{3III + III_{min}}{4III_{min}}\right]} \quad (18)$$

[1]No summation over i or j

with $C_s = 50$, $III = b_{ik}b_{kj}b_{ji}/3$ where $b_{ij} = \overline{u_i u_j}/2k - \delta_{ij}/3$ and $III_{min} = -1/108$. This modification is not effective in the wall region. Further out when III becomes less than $III_{min}/3$, L will be reduced. The modified length scale has a theoretical minimum of approximately 1/2 of the Kolmogorov scale for symmetric two-dimensional turbulence. Model constants used are listed in table 1.

$C_{\varepsilon 1}$	$C_{\varepsilon 2}$	C_μ	σ_ε	C_L	C_η	C_s	a_1
1.40	1.83	0.26	1.40	0.20	90	50	0.10

Table 1: Model constants

Other turbulence models

For comparison we have tested a range of turbulence models, starting with a simple mixing-length model, with mixing-length given as (van Driest, 1956)

$$l = \kappa y \left[1 - \exp(-y u_* / \nu A^+)\right] \qquad (19)$$

with $\kappa = 0.40$ and $A^+ = 26$.

The Launder & Sharma (1974) k-ε-model and the k-ε-v^2-model proposed by Durbin (1991) have also been tested. Here the IP model was used in the f_{22}-equation. Results are shown in figure 9.

CHANNEL FLOW RESULTS

To test the modifications of the elliptic relaxation formulation we simulated the flow between to infinite planes at $Re_\tau = 180$ and $Re_\tau = 590$ and compared the results with DNS data (Moser et al., 1999). The turbulence intensities (Fig 2 & 3) and the velocity profiles, (Fig 4) scaled with u_*, coincide well with DNS results for both Reynolds numbers, demonstrating that the new formulation is adequate for wall-bounded flows.

FILM FLOW RESULTS

Figure 5 shows turbulence intensities for film flow with the original length scale (eq. 9) and the modified length scale (eq. 18). Here Durbin's original elliptic relaxation formulation is used. By employing the original length scale, $\overline{u_2 u_2}$ is over-damped towards the surface. The energy of $\overline{u_2 u_2}$ is redistributed to the other components approaching the surface, but since $\overline{u_2 u_2}$ contains relatively little energy no enhancement of $\overline{u_1 u_1}$ or $\overline{u_3 u_3}$ in the surface region can be seen. With the modified length scale we observe an increase in $\overline{u_3 u_3}$ approaching the surface, which is in accordance with

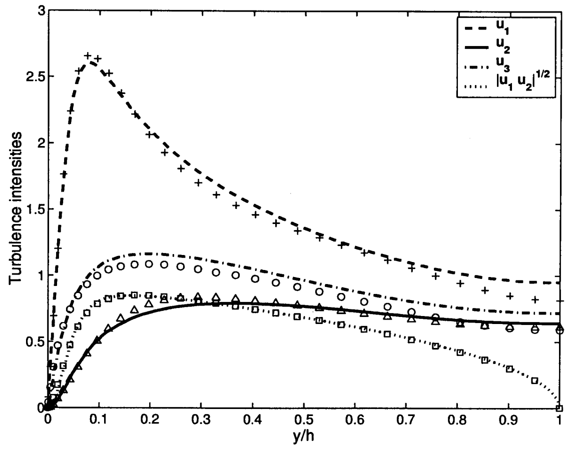

Figure 2: Turbulence intensities in channel flow at $Re_\tau = 180$, model (lines) and DNS (symbols).

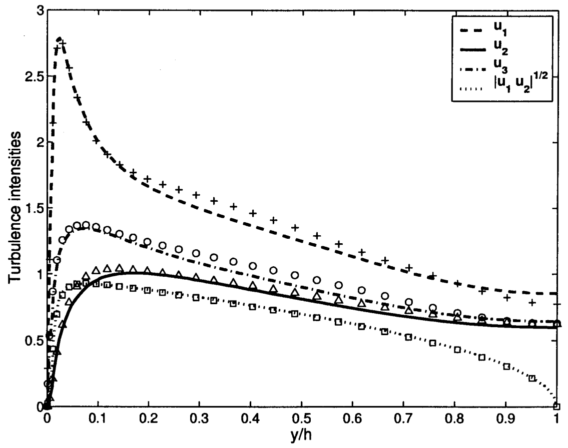

Figure 3: Turbulence intensities in channel flow at $Re_\tau = 590$, model (lines) and DNS (symbols).

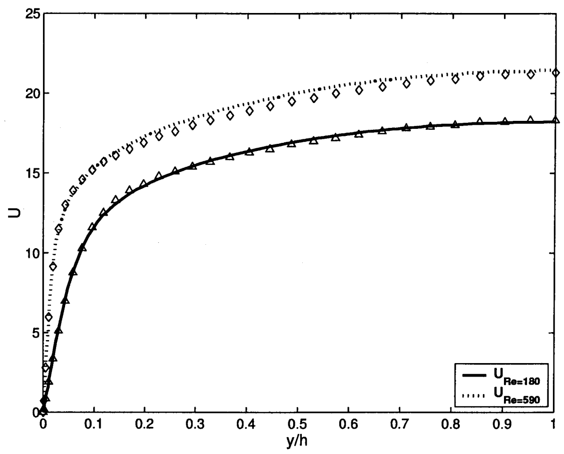

Figure 4: Mean velocity profiles in channel flow at $Re_\tau = 180$ and $Re_\tau = 590$, model (lines) and DNS (symbols).

experiments (Komori & Ueda, 1982) and DNS (Lam & Banerjee, 1992).

Figure 6 compares the redistribution term, $\wp_{ij}$, with the original and the modified length scale. With the modified length scale the process of withdrawing energy from the nor-

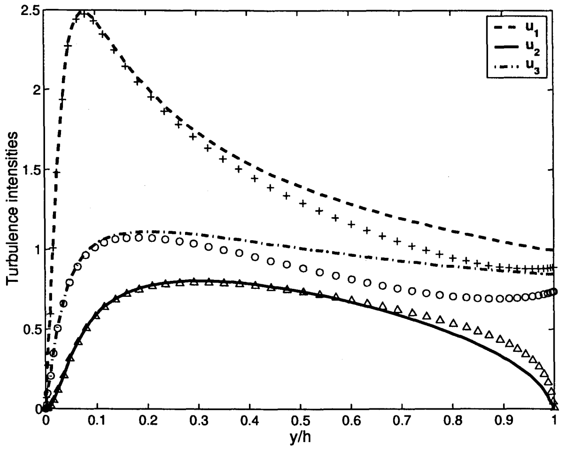

Figure 5: Turbulence intensities in film flow at $Re_\tau = 180$. Original (lines) and modified elliptic length scale (symbols).

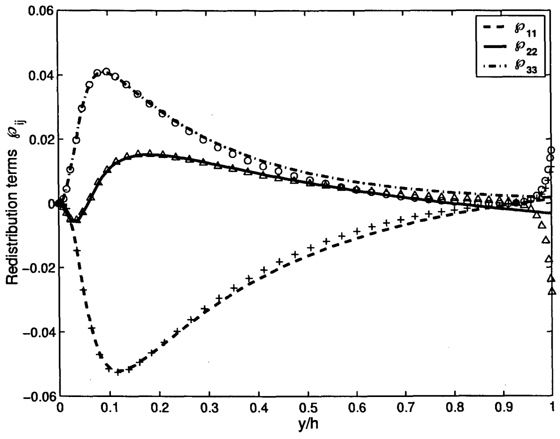

Figure 6: Redistribution terms $\wp_{ij}$ in film flow at $Re_\tau = 180$. Original (lines) and modified (symbols) elliptic length scale.

mal component is concentrated much closer to the surface, thereby increasing the energy of $\overline{u_3 u_3}$. While $\wp_{ij}$ performs the redistribution, the physically incorrect nonzero of $\wp_{22}$ at the surface is glaring.

Modified relaxation equation

The turbulence intensities from the simulation with the new elliptic relaxation formulation is presented in figure 7 together with experimental results (Komori & Ueda, 1982) on film flow at $Re_\tau = 194$. The results for normal and streamwise components agree very well with the experiments. The model predicts considerably higher intensity of the spanwise component than the experiments. This might partly explain why the increase in $\overline{u_3 u_3}$ towards the surface is underestimated by the model. The normal component has not enough energy to considerably increase the spanwise component.

The redistribution term, $\wp_{ij}$, with the new formulation (Fig 8) behaves very nobly towards

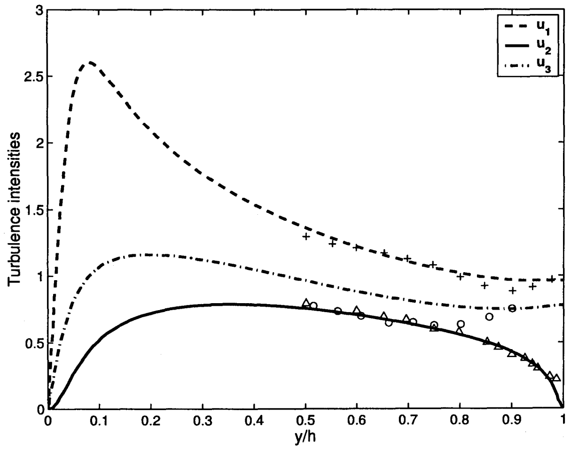

Figure 7: Turbulence intensities in film flow, new model formulation at $Re_\tau = 180$ (lines) and experiments (Komori & Ueda, 1982) at $Re_\tau = 194$ (symbols).

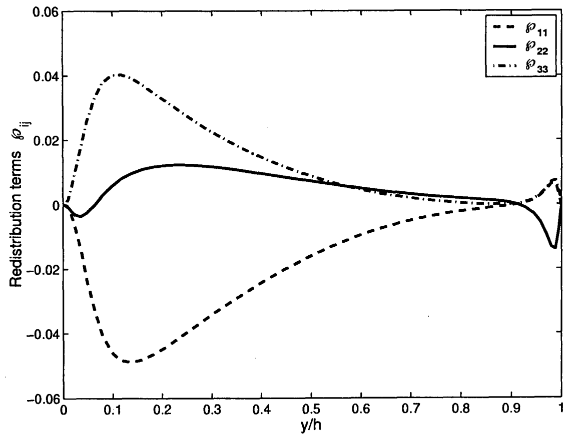

Figure 8: Redistribution terms $\wp_{ij}$ in film flow at $Re_\tau = 180$. New elliptic relaxation model formulation.

the surface and in full accordance with the DNS data by Komori et al. (1993). $\wp_{22}$ and $\wp_{12}$ (not shown here) are both zero on the surface, whereas $\wp_{11}$ and $\wp_{33}$ attain a small negative and positive value, respectively. With this formulation, the energy is equally redistributed between the streamwise and spanwise component. Compared to the original formulation the process of distributing energy from $\overline{u_2 u_2}$ to the other components is expelled away from the surface to the region just below, thus evading the unphysical situation of a nonzero $\wp_{22}$ and $\wp_{12}$ at the surface.

Dimensionless film thickness h

Finally, figure 9 shows how the dimensionless film thickness h correlates with the film Reynolds number and how well the model predictions compare with the experimental data of Alekseenko et al. (1994) for a whole range of turbulence models. The k-ε model clearly overestimates the film thickness (or wall friction).

This is not surprising since no modification is introduced towards the surface. The simple mixing-length model gives better results than the k-ε model for this case. The SMC model with modified elliptic relaxation procedure and the k-ε-v^2 model conform nicely with the experiments.

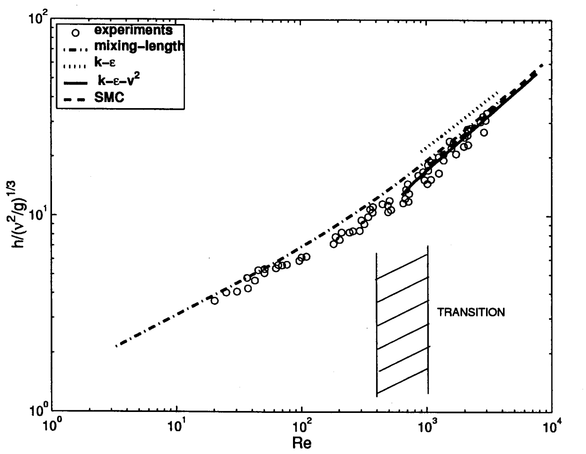

Figure 9: Dimensionless film thickness h versus film Reynolds number

CONCLUSION

Mixing-length and k-ε models in turbulent film flow simulations are sufficient for many engineering purposes. If more detailed information about the turbulence structure near the free surface is needed, i.e for heat transfer or chemical reactions, a more accurate model has to be adopted, like Durbin's k-ε-v^2 or a full second-moment model together with the elliptic relaxation procedure. The original formulation together with suitable boundary conditions works, but a glaring, physically wrong, nonzero value of the normal redistribution term on the free surface has been observed. This shortcoming is remedied with the new formulation proposed in this article. The new formulation does neither enhance the complexity of the model nor aggravate the near-wall behaviour of the redistribution term $\wp_{ij}$.

REFERENCES

Alekseenko, S.V., Nakoryakov, V.E., and Pokusaev, B.G., 1994, *Wave Flow of Liquid Films*, Begell House.

Daly, B. I., and Harlow, F.H., 1970, "Transport equations of turbulence", *Phys. Fluids*, Vol. 13, pp. 2634-2649.

Dreeben, T. D., and Pope, S. B., 1997, "Probability density function and Reynolds-stress modeling of near-wall turbulent flows", *Phys. Fluids*, Vol. 9, pp. 154-163.

Driest, E. R. van, 1956 "On Turbulent Flow Near a Wall", *J. Aero. Sci.*, Vol. 23, pp. 1007-1011.

Durbin P. A., 1991, "Near-wall turbulence closure modeling without damping functions", *Theo. Comp. Fluid Dyn.* Vol. 3, pp. 1-13.

Durbin P. A., 1993, "A Reynolds stress model for near-wall turbulence", *J. Fluid Mech*, Vol. 249, pp. 465-498.

Fulford, G.D., 1964 "The flow of liquids in thin films", *Adv. Chem. Eng.*, Vol. 5, pp. 151-236.

Gibson, M. M., and Rodi, W., 1989, "Simulation of free surface effects on turbulence with a Reynolds stress model", *J. Hydraulic Res.*, Vol. 27, pp. 233-244.

Komori, S., and Ueda, H., 1982, "Turbulence structure and transport mechanism at the free surface in an open channel flow", *Int. J. Heat Mass Transfer*, Vol. 25, pp. 513-521.

Komori, S., Nagaosa R., Murakami Y., Chiba, S., Ishii, K., and Kuwahara, K., 1993, "Direct numerical simulation of three-dimensional open-channel flow with zero-shear gas-liquid interface", *Phys. Fluids A*, Vol 5, pp. 115-125.

Lam, K., and Banerjee S., 1992, "On the condition of streak formation in a bounded turbulent flow", *Phys. Fluids A*, Vol. 4, pp. 306-320.

Launder, B. E., and Sharma, B. I., 1974, "Application of the energy-dissipation model of turbulence to the calculation of flow near a spinning disk", *Lett. Heat Mass Transfer*, Vol. 1, pp. 131-138.

Moser, D. R., Kim, J., and Mansour, N. N., 1999, "Direct numerical simulation of turbulent channel flow up to Re_τ=590", *Phys. Fluids*, Vol. 11, pp. 943-945.

Speziale, C. G., Sarkar, S., and Gatski, T. B., 1991, "Modelling of the pressure-strain correlation of turbulence: an invariant dynamical systems approach", *J. Fluid Mech.* Vol. 227, pp. 245-272.

Wizman, V., Laurence, D.,Kanniche, M., Durbin, P., and Demuren, A., 1996, "Modeling near-wall effects in second-moment closures by elliptic relaxation", *Int. J. Heat Fluid Flow*, Vol. 17, pp. 255-266.

Yih, S.-M., and Liu, J.-L., 1983, "Prediction of heat transfer in turbulent falling films with or without interfacial shear," *AIChE J.* Vol. 29, pp. 903-909.